



Sustainable 3D printing with alkali-treated hemp fiber-reinforced polycarbonate composites

İrem Ceylan · Neşe Çakıcı Alp · Ayşe Aytaç

Received: 22 September 2023 / Accepted: 8 April 2024
© The Author(s) 2024

Abstract The study investigated the properties of alkali-treated hemp fiber-reinforced polycarbonate (PC) composites that can be formed by 3D printers for architectural applications. To determine the optimum alkali treatment to be applied to the fibers, the properties of the samples treated with 5% and 7% sodium hydroxide (NaOH) at both ambient temperature (AT) and 120 °C (HT) were determined by Fourier transform infrared spectroscopy (FTIR) and thermogravimetric analysis (TGA). It was determined that the alkali treatment that gave the optimum result was 5% HT. Composite specimens with fiber/matrix ratios of 10/90, 20/80, and 30/70 were prepared in filament form to be printed in a 3D printer as alkali-treated and untreated. These composites were characterized by conducting tensile strength, FTIR, differential scanning calorimetry (DSC), TGA, and scanning electron microscopy (SEM) analyses. Tensile strength

results revealed the highest mechanical performance for 5% NaOH alkali-treated and 10 wt.% hemp fiber-reinforced PC composites. DSC results showed that slight changes occurred in the glass transition temperature values. Furthermore, SEM analysis showed that 5% NaOH-treated hemp fibers have better interfacial bonding with the PC matrix than untreated fibers. As a result, more natural and sustainable materials have been obtained for architectural applications without significantly decreasing in PC properties.

Keywords 3D Printer materials · Alkali-treated-hemp fiber · Polycarbonate · FDM

Introduction

Traditional synthetic fiber-reinforced polymer composites (FRPC), mainly glass, aramid, and carbon fibers, have been used for fifty years. FRPC is the term used for fiber-reinforced polymer composites (Azwa and Yousif 2013) and is often used in the transportation, aerospace, automobile, and construction industries (Kandola et al. 2021; Thakur et al. 2017). Although composites reinforced with synthetic fibers are preferred in these applications because of their high strength-to-weight ratios, studies on composites reinforced with natural fibers have come to the fore to reduce environmental damage concerning carbon footprint, sustainability, and recycling. These concepts have been on the agenda of the global economy

Present Address:

İ. Ceylan · N. Çakıcı Alp
Department of Architecture, Architecture and Design
Faculty, Kocaeli University, 41380 Kocaeli, Turkey
e-mail: 186144006@kocaeli.edu.tr; iremceylan-@hotmail.com

A. Aytaç
Department of Chemical Engineering, Engineering
Faculty, Kocaeli University, 41380 Kocaeli, Turkey

A. Aytaç
Polymer Science and Technology Programme, Kocaeli
University, Kocaeli, Turkey

and the world in recent years. Interest in natural fiber reinforced polymer composite materials is growing rapidly in industrial applications and scientific research. In terms of sustainability and reducing environmental damage, natural fibers are preferred for widespread application because they are abundant in nature, are fully or partially biodegradable, have low costs, and are an ecological alternative with satisfactory mechanical properties compared to synthetic fibers such as glass fibers (Kozłowski and Władysław Przybylak 2008).

Using natural fibers allows for less extraction power and greener, sustainable, and smarter construction development than polymer/steel/synthetic fibers (Juárez et al. 2010; Saba et al. 2016). Thermoplastic composites reinforced with natural fibers are known to be more energy-efficient and sustainable alternatives to traditional materials with low density, good thermal and acoustic insulation, CO₂ sequestration enhanced mechanical properties, reduced tool wear in machining operations, and problem-free disposal (Alves et al. 2010; Ayırmis et al. 2011; Jhanji Dhir 2022). In addition, natural fiber-reinforced polymer composites (NFRPCs) have better electrical and higher fracture resistance (Sanjay et al. 2018). NFRPCs are easy to form, cost efficient, have low energy requirements, safe for health, lightweight, have high stiffness, and can be an alternative to FRPCs in various applications (Saba et al. 2015). Natural fibers are used as reinforcing materials for polymer-based matrices (Faruk et al. 2012). These polymer-based matrices are categorized thermosetting plastics, and thermoplastics (Kozłowski and Władysław Przybylak 2006). Thermoplastics can be processed and molded under various temperatures without undergoing chemical or bond changes in the polymer chain. Therefore, they are critical materials for recycling and, therefore, sustainability (Wang et al. 2003). Natural fibers used matrices such as polyethylene (Li et al. 2009), PLA (Hu and Lim 2007), polypropylene (Ku et al. 2011), polystyrene (Zafar and Siddiqui 2020), polyvinyl chloride (PVC) (Wirawan et al. 2009), and polycarbonate (PC) (Karsli and Aytac 2014). Among these polymers, PC is known to have high impact strength, high elastic modulus, high heat deflection temperatures, and very low moisture absorption (Vinyas et al. 2019) and has many applications in the construction sector. The literature indicates that the natural fibers used to reinforce the PC

matrix are wood shavings (Wimonsong et al. 2012; Zhang et al. 2020, 2021), tamarind fruit (Maheswari et al. 2012), *Cordia dichotoma* (Jayaramudu et al. 2013), pineapple leaf fiber (Threepopnatkul et al. 2009), silk and cotton (Taşdemir et al. 2008), and flax (Karsli and Aytac 2014; Panthapulakkal and Sain 2013).

Cellulosic fibers such as hemp, flax, jute, sisal, coir, bamboo, banana, kenaf, and ramie are used as reinforcement in NFRPCs and are abundant in many countries (Yan et al. 2016). Lignocellulosic fibers such as jute, sisal, flax, and hemp have been reported to be an alternative to glass-fiber and carbon-fiber-reinforced composites in various applications (Faruk et al. 2012; Kandola et al. 2021). The mechanical and dynamic mechanical properties of polymer composites reinforced with kenaf, jute, and hemp fibers are suitable for use in building structures (Saba et al. 2015). Besides, NFRPCs are used as ceiling panels, partition boards, and fiber boards in various structural applications (Kozłowski and Władysław Przybylak 2008; Nishino et al. 2003) as well as window and door frames and furniture applications (Sanjay et al. 2018). When it comes to hemp fiber, it is known to have a 3–9 times faster growth rate than other plants and a higher CO₂ absorption capacity than any other plant. In addition, it can be planted in various areas and requires very little fertilizer and herbicides (pesticides) (Amaducci et al. 2015), grows very fast, yields more fiber per acre compared with kenaf and flax (Liu et al. 2017). Therefore, using hemp fiber for NFRPCs will create a greener and more sustainable alternative, and the damage to nature will be minimized. When the studies in the literature dealing with thermoplastic composites reinforced with hemp fiber are examined, PLA, polyethylene, and polypropylene are chosen as the matrix (Bourmaud and Baley 2007; Hapuarachchi and Peijs 2010; Pickering et al. 2011; Sawpan et al. 2011; Sunny et al. 2020; Szostak et al. 2019).

For sustainability, reducing environmental damage and reducing CO₂ emissions, the natural fiber content of the used material, and the production and application of the material are important. According to studies in the literature, it has been determined that cumulative energy is reduced by 41–64% in the production of polymer-based materials produced with 3D printers (Kreiger and Pearce 2013). Besides, NFRPCs produced with 3D printers are known to reduce carbon dioxide emissions and carbon footprint compared

with traditional production techniques (Mohammed et al. 2017; Victoria Santos et al. 2022). In 3D printing, i.e., additive manufacturing (AM), the designed parts are produced in layers, rather than subtracting from a larger part. One of the production techniques used in AM technology is fused filament fabrication, which is obtained by extruding thermoplastic or wax material from a heated nozzle. Other manufacturing techniques include jetting a binder into a polymeric powder, using an ultraviolet laser to harden a photosensitive polymer, and using a laser to melt polymeric powder (Laser Sintering) (Williams and Ivanova 2011). The most used production type in AM technology is fused deposition modeling (FDM), and versatile structural parts can be produced with minimal waste material without the need for investments such as molds, huge machines, and excess staffing for rapid prototyping (RP) (Hashemi Sanatgar et al. 2017; Vinyas et al. 2019).

3D printing is used to apply computer-aided design (CAD) files of 3D objects, which are digitally designed for use in different applications or obtained by scanning an existing object through therapeutic prototyping or rapid manufacturing. Thanks to 3D printing technology, it is possible to create low-cost, rapid design solutions and applications and eliminate defects at early design stages (Chua et al. 2003; Williams and Ivanova 2011). 3D printed parts are characterized as anisotropic and depend on the direction of printing and raster angle. In addition, their mechanical properties and structural strength depend on many factors, such as extrusion speed, nozzle, bed temperature, and infill ratio (Domingo Espin et al. 2015). The most used thermoplastic polymers in FDM technology are ABS, PLA, PC, and PET-G. Considering the fiber-reinforced thermoplastics produced with FDM technology, ABS and PC have the best structural integrity and are used in many engineering applications where strength is important (Vinyas et al. 2019).

To the best of the authors' knowledge, although there are a few studies in which the polycarbonate matrix is reinforced with hemp fiber, no study has been conducted on with these composite materials using the 3D printing production technique. Therefore, this study will uniquely contribute to the literature by producing hemp fiber-reinforced polycarbonate composites by 3D printing. The fact that hemp fiber-reinforced PC composites are suitable for use in 3D printers will contribute to the concept of

sustainability by reducing environmental damage. In terms of architecture, the designer starts the design and production process by making his/her imagination visible with CAD. Although the freedom of design with CAD is unlimited, the materials used can be given limited forms due to traditional production techniques. With the direct production of CAD files using a 3D printer, complex forms that cannot be made using conventional production techniques can be applied more easily in architecture and building applications. Because the material produced within the scope of this study is suitable for 3D printers, the designer can have freedom and pave the way for architectural applications in complex forms. Therefore, this study aims to determine the optimal composite ratio of hemp fiber-reinforced polycarbonate composite, which can be shaped with a 3D printer, for use in architectural applications. Therefore, samples were prepared using an extrusion stage and a 3D printer. Thermal (DSC, TGA), chemical (FTIR), mechanical (tensile test), and morphological (SEM) properties of the composite samples were tested by the standards to determine the optimal composite blend ratio and ease of application in 3D printers.

Experimental

Materials

Pure PC was used as a control sample. PC suitable for general use was supplied by Lotte Chemical and used as the matrix material (specific gravity 1.20, Tensile Strength: 63–70 MPa, elastic modulus: 2400–2500 MPa, impact strength: 80–85 kJ/m², deformation temperature: 130°C, Vicat softening temperature: 150 °C, MFI (fluidity index): 10). The hemp fibers used are from Hemp Traders of America and are in raw form, degummed, and have lignin not removed (see Fig. 1). The fibers were aligned in the same direction. Sodium hydroxide (NaOH) was obtained from Katki Dunyasi and is 99% pure.

Methods

The experimental study was conducted in two stages. The first stage is described under the title 'Surface Treatment of Hemp Fibers,' the optimum alkali treatment to be applied to the fibers was determined by



Fig. 1 Supplied raw hemp fiber bundle

looking at their chemical and thermal properties using FTIR and TGA analysis. The second stage is described under the title '3D printed composites', and PC/hemp composite samples with different ratios were produced by applying the specified alkali treatment. The sample with the best chemical, thermal, mechanical, and morphological properties suitable for use in a 3D printer was determined using FTIR, TGA, DSC, SEM, and tensile tests.

Surface treatment of hemp fibers

Although NFRPCs have many advantages and application areas, they also have disadvantages such as water absorption, strength degradation, lack of thermal stability, lowered impact properties, and reduced impact strength due to weak matrix interface bonding when applied directly due to their hydrophilic structure. Alkaline, silane, and acetylation chemical treatments were performed to overcome these disadvantages. These chemical treatments improve the interfacial bonding between hydrophilic fibers and hydrophobic (water-avoidance) polymers, thereby reducing moisture uptake, increasing microbial degradation resistance, and extending durability (Liu et al. 2017). Alkali treatment, or mercerization, is one of the most widely applied chemical treatments to natural fibers that reinforce thermoplastics. As a result of the alkali

treatment, the surface hardness is increased by removing the hydrogen bonding in the network structure. In addition, substances such as lignin, wax, and oils on the fiber surface are removed, and the natural cellulose structure is depolymerized, resulting in short-length crystallites (Mohanty et al. 2001; Wang et al. 2003). This way, the material's properties are improved by providing a better interfacial bond between the natural fiber and the thermoplastic matrix. According to the literature, optimum results have been obtained from the alkaline treatment of hemp fiber with NaOH solution (Bhoopathi and Ramesh 2020; Rachini et al. 2009; Suardana et al. 2011). Therefore, in this study, NaOH was chosen for the alkali treatment. The NaOH alkaline treatment will reduce the lignin and hemicellulose, increase the cellulose content of hemp fibers, balance the hydrophilic structure, and provide a better interface bond with PC. As a result, the fiber surfaces will become clean and rough, and the molten polycarbonate will provide better mechanical locking with the fibers.

To determine the optimum NaOH alkali treatment to be applied to hemp fibers within the scope of the study, 5% and 7% (NaOH/pure water) solutions were applied in four different ways, namely heat treatment (HT) and ambient temperature (AT). The samples processed under AT conditions were stirred at 200 rpm in an IKA C-MAG HS 7 device for 60 min at room temperature and then washed in tap water for 5 min to remove the solution from the fibers and neutralize it. The washed fibers were left to dry overnight at room temperature and then dried at -0.6 bar pressure and 80 °C for 24 h to remove residual moisture. The samples processed under HT conditions were stirred at 120 °C for 60 min at 200 rpm in a DATHAN SCIENTIFIC MSH-20D device and then washed in tap water for 5 min to remove the solution in the fibers and neutralize it. The washed fibers were left to dry overnight at room temperature and then dried at -0.6 bar pressure and 80 °C for 24 h to remove residual moisture. The fibers used in the control sample were soaked in pure water for 24 h to remove impurities, and the same drying process was used. TGA analysis was performed to determine the thermal properties, and FTIR analysis was performed to determine the chemical properties of the NaOH-treated and untreated samples. The fiber samples are coded according to the hemp fiber they contain, and

Table 1 Alkali-treated and untreated samples

Sample	NaOH (%)	Pure Water (%)	Processing Condition
HEMP0	0	100	24 h Pure Water
HEMP5AT	5	95	AT
HEMP5HT	5	95	HT
HEMP7AT	7	93	AT
HEMP7HT	7	93	HT

the process applied, as shown in Table 1. For example, the code HEMP5HT indicates a fiber sample treated with 5% NaOH at 120 °C.

3D-Printed composite preparation

Within the scope of this study, the Anycubic 13 3D printer was chosen to apply the additive manufacturing method. Hemp fiber-reinforced composite samples were prepared as filaments with a 1.00–2.00 mm diameter in the Twin-Screw Extruder device. The composite samples were prepared with 10%, 20%, and 30% fiber ratios, alkali-treated and untreated, and pure PC was used as a control sample. Hemp fibers were cut into 6 mm lengths and prepared as alkali-treated and untreated. Alkaline treated fibers were treated in 5% NaOH solution under HT conditions, washed in tap water until the pH was neutral, and left to dry overnight. The untreated fibers were soaked in pure water for 24 h and left to dry overnight at room temperature. The dried fibers and PC pellets were dehumidified in a Witeg oven at 80 °C with -0.6 bar pressure for 24 h. The dehumidified fiber and matrix materials were weighed at 10/90, 20/80, and 30/70 PC/Hemp ratios and prepared for use in the twin-screw extruder device. The materials were mixed in the twin-screw extruder at a speed of 100 rpm and a temperature of 250 °C. The materials were fed into the extruder via the feed hopper and mixed as a melt at the determined ratios (see Table 2). At first, PC pellets were fed to the extruder barrel and mixed for 2 min, then fibers were fed, and the mixing time was continued for another 1 min. After mixing for 3 min, including the fiber feeding time, filaments with a diameter of 1.0–2.0 mm were obtained. The obtained filaments were printed in triplicate, each with dimensions of 75 × 12 × 2 mm, for use in the tensile test with

Table 2 Compounding ratios of the composites

Sample	5% NaOH Treated Hemp Fiber (%)	Untreated Hemp Fiber (%)	PC (%)
PC	0	0	100
PCH10	0	10	90
PCH20	0	20	80
PCH30	0	30	70
PCH105HT	10	0	90
PCH205HT	20	0	80
PCH305HT	30	0	70

Anycubic 13 3b printing device (Figs. 2 and 3). The printing parameters are given in Table 3.

Characterization

The FTIR spectrum measures the wavelengths of electromagnetic light against its infrared intensity. The range of wavelengths indicates components such as cellulose, hemicellulose, lignin, waxy structure, methylene group, and their chemical bonds. For better interfacial bonding of fiber and matrix material, lignin, methylene group, waxy structure, and hemicellulose should be removed, and the cellulose and -OH density should be increased. Therefore, in this study, the increase and decrease in these components resulting from different alkali treatments applied to the fibers and composites were determined by FTIR spectroscopy. The alkali treatment method that gives the most optimum results will be determined for use in composite production. In addition, FTIR spectra were performed to determine the chemical properties of the produced composite samples. FTIR analysis was repeated twice to check the data. The FTIR spectra measurements made within the scope of the study were performed under a nitrogen atmosphere using the Spectrum IR program with a wavelength of 4000 cm⁻¹–650 cm⁻¹.

Thermogravimetry analysis determines the mass loss of materials as a function of temperature or time. The sample was heated to a set temperature at a constant heating rate, and the mass change was measured and recorded as a function of time. Mass change indicates thermal degradation and occurs at different temperature stages for other materials. This study carried out TGA analysis on fibers and composite samples.

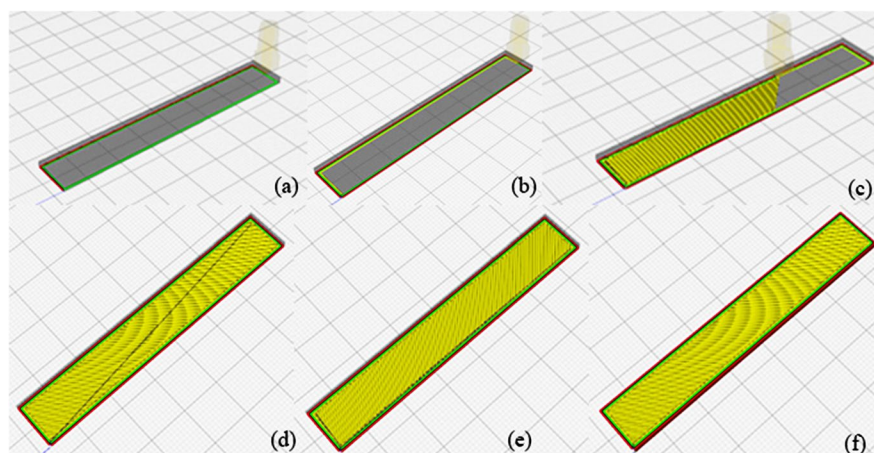


Fig. 2 3D printing previsualizes the sample to be printed in the Ultra Maker Cura program. (a) inner wall (green) and shell (red); (b) addition of a filling layer (yellow) to the inner wall and shell; (c) line pattern fillings of the first layer filled at +45°

angle, (d) line pattern fillings of the second layer filled at an angle of -45°, (e) line pattern fillings of the third layer filled at an angle of +45°, (f) line pattern fillings of the 18th layer (last layer) filled at an angle of -45°



Fig. 3 A 3D printed composite sample

Table 3 3D printing parameters

3D Printing Parameters	
First layer height (mm)	0.3
Layer height (mm)	0.1
Layer width (mm)	0.4
Filling pattern	Line
Filling ratio (%)	100
Fill alignment (degree, angle)	45
Shell thickness (mm)	1.0
Number of shells	2
Printing speed (mm/s)	30.0
Nozzle diameter (mm)	1.0
Print temperature (°C)	260
Bed temperature (°C)	110

TGA analysis was repeated twice to verify the data. The Mettler Toledo MTTA18110856 TGA 1 device was used for TGA analysis and tested under a nitrogen atmosphere. TGA analysis was performed at a temperature range of 25 °C -600 °C, with a heating rate of 10 °C/min and a 30 ml/min nitrogen flow. The sample weights of approximately 10 mg were placed in a ceramic pan in the device.

Differential scanning calorimetry (DSC) is a thermal analysis technique that examines how the heat capacity of a material changes with temperature. In this study, DSC analysis was applied to composite samples and was repeated twice to verify the data. DSC analysis was performed with a Mettler Toledo DSC machine using nitrogen gas. Aluminum pans were prepared for machine testing. Samples in the pans were prepared at 5–10 mg. A two-stage analysis was determined as the test method with a 10 °C/min temperature increase between 25–250 °C. After the samples were heated from 25 °C to 250 °C, the analysis was completed by cooling down to 25 °C and then increasing to 250 °C again. In the first heating stage, the thermal traces left by the twin-screw extruder were erased, and the results of the second heating stage will be considered. T_g values of the samples were determined.

In the tensile test, the tensile strength values were examined. Tensile strength indicates the maximum force that can be withstood until it breaks or fractures

and is important in architectural applications. The tensile test within the scope of the study was applied to three bars of $75 \times 12 \times 2$ mm from each composite specimen. Composite specimens were tested in an Instron Tensile Machine with 6 bar pressure using the Instron Bluehill Universal program with the ISO 527-5A 10 mm/min method, and their mechanical properties were determined.

The morphology of the produced composite samples was determined using an electron microscope (SEM, Quanta FEG 450). The device was used in the secondary electron mode at a 15.00 kV current and 4.48×10^{-4} Pa pressure. The zoom ratio is 100, 500, and 1000. The samples used in the SEM analysis were obtained from tensile tests of composite samples produced by the FDM technique. Because the samples are polymer-containing insulating materials, they are

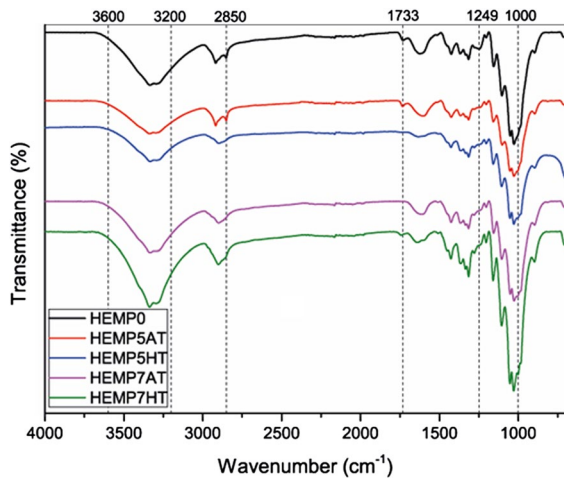


Fig. 4 FTIR spectra obtained from the fibers

Table 4 FTIR spectra of the alkali-treated and untreated fibers

Wave number (cm ⁻¹)	Associated Chemical Groups	HEMP0	HEMP5AT	HEMP5HT	HEMP7AT	HEMP7HT
1000	-OH density	Low	Higher	Highest	Higher	Highest
1249	C=O (lignin)	Predominant	Removed	Removed	Removed	Removed
2850	Methylene group	Present	Increased	Removed	Removed	Removed
1733	C=O (Pectin, methyl ester, waxy structure)	High	High	Removed	Removed	High
3200–3600	-OH stretching (cellulose)	Low	Increased at a low rate	Increased at a high rate	Increased at a low rate	Increased at a high rate

coated to make them conductive. The gold plating was applied for 90 s for conductivity under a voltage current of 10 m amperes.

Results and discussion

FTIR

The FTIR spectra of the NaOH-treated and untreated hemp fiber samples are shown in Fig. 4. The comparison of the chemical groups observed in the samples coded HEMP5AT, HEMP5HT, HEMP7AT, and HEMP7HT treated with alkali is presented comparatively with the HEMP0 sample in Table 4. The FTIR spectra of the NaOH-treated and untreated hemp fiber-reinforced PC composite samples are shown in Fig. 5.

According to Ouajai and Shanks (2005), the vibration at the 1733 cm^{-1} peak is attributed to the C=O stretching of methyl ester and carboxylic acid in pectin in hemp fibers (Ouajai and Shanks 2005). Kabir et al. (2012) also reported in their study on hemp fibers treated with alkali, silane, and acetylation processes that the peak value of 1737 cm^{-1} peak indicates C=O stretching (hemicellulose) (Kabir et al. 2012). The FTIR spectra of alkali-treated and untreated hemp fibers within the scope of the study (see Table 4.), a 1734.5 cm^{-1} peak was observed in HEMP0, HEMP5AT, and HEMP7HT samples. In the HEMP5HT and HEMP7AT samples, there was no 1734.5 cm^{-1} peak, and the sample with the minimum peak vibration was HEMP5HT. As a result, pectin and hemicellulose are best removed in the HEMP5HT and HEMP7AT samples.

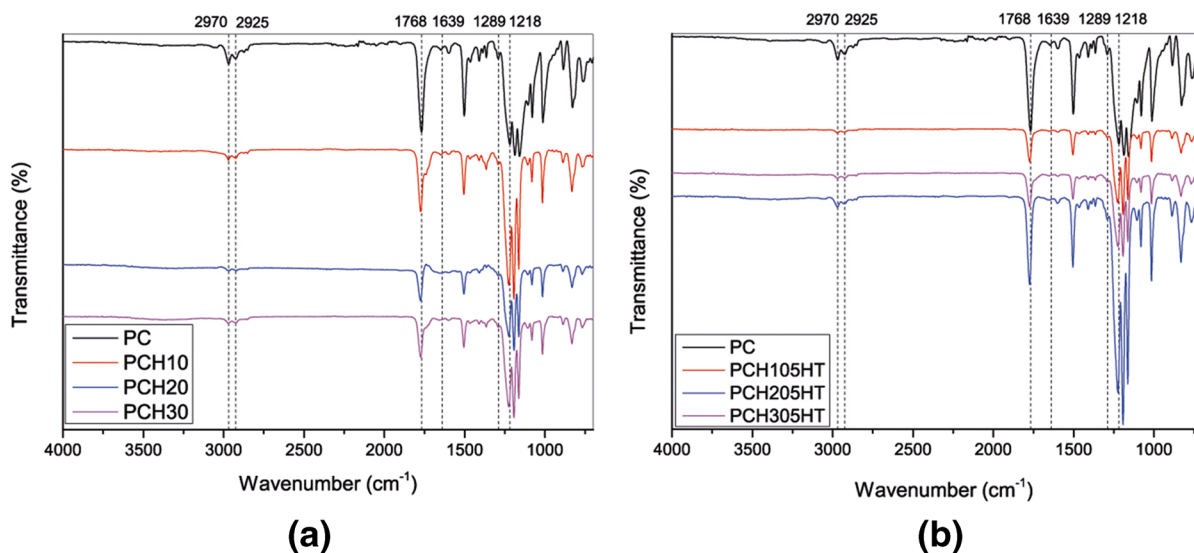


Fig. 5 FTIR spectra obtained from the composites reinforced with untreated (a) and alkali-treated (b) hemp fibers

Kabir et al. (2012) also stated that the 3407 cm^{-1} value indicates -OH stretching (cellulose) and found that cellulose was not removed because of alkali, silane, and acetylation processes (Kabir et al. 2012). When the cellulose peak values of the HEMP samples were analyzed, a peak of 3335 cm^{-1} was observed in the HEMP0 sample, and it was determined that the peak point was observed in the other samples, and cellulose remained. They also stated that a value of 1249 cm^{-1} indicates C=O stretching (lignin) (Kabir et al. 2012). Looking at the samples, lignin was observed in HEMP0 with a peak of 1243 cm^{-1} . In the alkali-treated HEMP5AT, HEMP5HT, HEMP7AT, and HEMP7HT samples, 1243 cm^{-1} peak value was not observed, and lignin was removed.

Lu and Oza (2013) stated that the 1000 cm^{-1} peak expresses the -OH density and that an increase in the peak will provide better interface bonding between the fiber and the thermoplastic matrix. They also stated that the 2850 cm^{-1} peak expresses the methylene group and is eliminated in alkaline-treated fibers (Lu and Oza 2013). The 1000 cm^{-1} peak showed an increase in the alkali-treated fibers at room temperature, and the highest increase was observed in the HEMP5HT and HEMP7HT samples. It was observed that the samples treated with alkali at temperature will provide better fiber–matrix interface bonding compared to those processed at room temperature. Looking at the 2850 cm^{-1} peak, it is seen

that it is eliminated in HEMP5HT, HEMP7AT, and HEMP7HT samples.

When the results of FTIR analysis of the alkaline treatment of fibers are considered, it is seen that lignin is generally removed in all alkali-treated samples. Pectin and hemicellulose were best removed in the HEMP5HT and HEMP7AT samples. The -OH density peak, which indicates better interfacial bonding between fiber and matrix material, was observed mainly in the HEMP5HT and HEMP7HT samples. Based on these data, it can be concluded that the HEMP5HT sample gives the most optimum result when used with matrix material.

According to Apaydin Varol et al. (2014), peak $2870\text{--}3054\text{ cm}^{-1}$ corresponds to C-H stretching, $1278\text{--}1326\text{ cm}^{-1}$ to C-H bending, and $584\text{--}741\text{ cm}^{-1}$ to C=O bending bonds (Apaydin-Varol et al. 2014). Peaks 2970 cm^{-1} (C-H stretching) and 1289 cm^{-1} (C-H bending) are observed in the pure PC sample, while a decrease is observed in the peaks in the PCH10 and PCH105HT samples. A slight decrease is observed in the C=O bending peak due to fiber addition. According to Haghghi Yazdi and Lee-Sullivan (2015), the carbonyl group occurs at a wavelength of 1760 cm^{-1} , and the C-O bond stretches from approximately $1150\text{ to }1250\text{ cm}^{-1}$. The methyl groups occur at wavelengths of $2850\text{ to }3000\text{ cm}^{-1}$ (Haghghi Yazdi and Lee-Sullivan 2015). Because of the FTIR test performed on pure PC within the scope of the study,

the carbonyl group was observed at peak 1768 cm^{-1} , stretching of the C-O bond at peak 1218 cm^{-1} , and a methyl group at peak 2970 cm^{-1} . When we examine the composites produced by adding fibers to PC, a significant decrease is observed in the carbonyl and methyl group peaks of the composites formed with both alkali-treated and untreated fibers. Stretching of the C-O bond is observed to increase because of fiber addition. According to Reddy et al. (2020), approximately 2925 cm^{-1} peaks correspond to α -cellulose, 1639 cm^{-1} absorbed water, and 1509 cm^{-1} aromatic C-H. The 2925 cm^{-1} peak was highest in pure PC and lowest in composite samples reinforced with alkaline fibers. The bonding of the NaOH alkali treatment with fibers can explain this phenomenon. Looking at 1639 cm^{-1} , a decrease is observed as fibers were added. The least amount of water absorbed was found in the composite samples reinforced with alkali-treated fibers. The 1509 cm^{-1} peak decreased slightly with the addition of fiber but remained dominant.

TGA analysis

The thermal degradation of natural fibers occurs in three main temperature stages. The first stage is, between $30\text{ }^{\circ}\text{C}$ and $110\text{ }^{\circ}\text{C}$, corresponds to removing moisture from the fibers (Kabir et al. 2012). The second is between $220\text{ }^{\circ}\text{C}$ and $280\text{ }^{\circ}\text{C}$, and the third is between $280\text{ }^{\circ}\text{C}$ and $300\text{ }^{\circ}\text{C}$. Degradation in the second range is associated with hemicellulose degradation, whereas that in the third range is lignin

degradation. The activation energies in the second and third stages are 25 and 35 kcal/mol, respectively, corresponding to hemicellulose and lignin degradation. The degradation of natural fibers is crucial for constructing natural fiber composites and effectively withstanding the curing temperature for thermosets and the extrusion temperature for thermoplastic composites (Nabi and Jog 1999). To determine the weight loss of the samples at $30\text{ }^{\circ}\text{C}$ - $110\text{ }^{\circ}\text{C}$ for moisture removal, $220\text{ }^{\circ}\text{C}$ - $280\text{ }^{\circ}\text{C}$ for hemicellulose degradation, and $280\text{ }^{\circ}\text{C}$ - $300\text{ }^{\circ}\text{C}$ for lignin degradation, the remaining weight percentages against temperature values are given in Fig. 6 and Table 5. According to Oza et al. (2014), weight loss between 6 and 8% indicates the moisture content of the fiber (Oza et al. 2014). From this viewpoint, moisture removal was achieved in all samples between $30\text{ }^{\circ}\text{C}$ and $110\text{ }^{\circ}\text{C}$. When we look at the residual weights after hemicellulose degradation ($280\text{ }^{\circ}\text{C}$), the highest residue value is seen in the HEMP5HT sample with a value of 92.5703%. After lignin degradation ($300\text{ }^{\circ}\text{C}$), the highest residue amount was observed in the HEMP5HT sample at 91.4375% (see Fig. 6). At approximately $600\text{ }^{\circ}\text{C}$, the highest residue value was observed in the HEMP0 sample at 23.98% and the lowest in the HEMP5HT sample at 15.73% (see Table 5.).

The reported studies in the literature show that degradation starts at higher temperatures, and thermal stability increases in alkali-treated fibers (Pracella et al. 2010). The increase in thermal stability

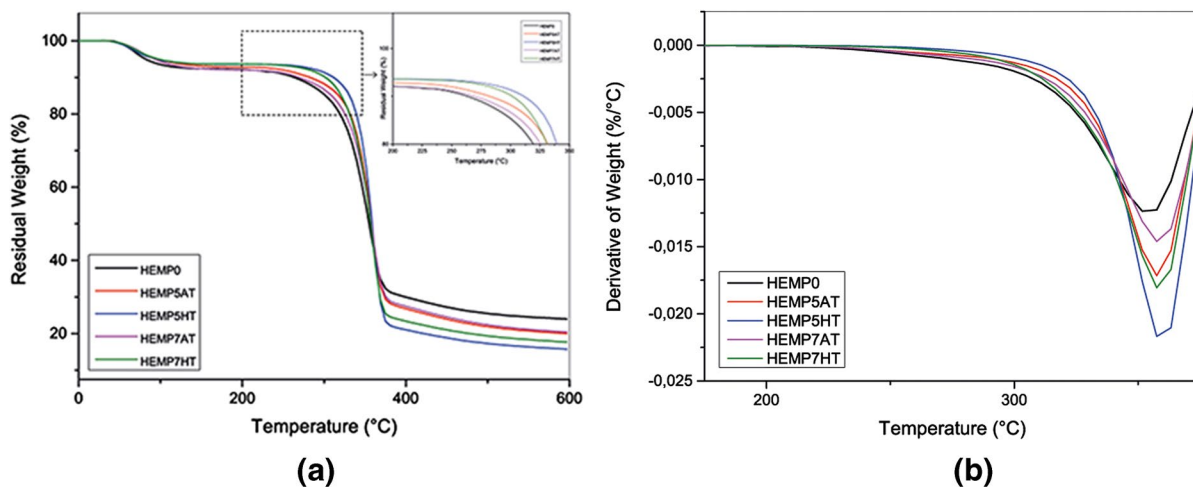


Fig. 6 TGA (a) and DTG (b) thermograms of fibers

is attributed to removing of lignin, waxy structure, and oils covering the fiber surface by alkaline treatment (Vinyas et al. 2019). Looking at the peaks of the DTG curve obtained within the scope of the study (see Table 3.), it is seen that while the maximum degradation temperature peak in untreated fibers is 354.65 °C, the highest temperature peak in treated fibers (HEMP5HT) reaches 359.98 °C. The increase in this value is similar to the alkaline treatments applied to hemp fibers in the literature (Pracella et al. 2010). The alkaline treatment is expected to harden the fiber surface. This removes the waxy structure, pectin, hemicellulose, and lignin to reveal more cellulose and improve the mechanical bond between the fiber and polymer (Oza et al. 2014). At the temperature at which 10% weight loss occurs,

the HEMP5HT sample shows an improvement of 18% compared with the untreated fibers, which is higher than the other samples. Considering the data obtained from the FTIR analysis, the HEMP5HT sample appears to be the best choice for reinforcing the PC composite. Therefore, the HEMP5HT sample was selected to reinforce PC in composite production (Table 6).

The TGA and derivativeweight (DTG) curves of the composite samples, including alkali-treated and untreated fibers, are shown in Fig. 7, and the heat-induced mass loss values are summarized in Table 7. According to the TGA analysis, alkaline treatment of the fibers increased the thermal strength. This situation was supported by studies reported in the literature.

Table 5 Heat-induced mass loss because of the TGA analysis of fiber samples

Sample	5% Weight Loss (°C)	10% Weight Loss (°C)	50% Weight Loss (°C)	600 °C Residue (%)
HEMP0	81.62	263.22	255.07	23.98
HEMP5AT	95.04	282.51	358.01	19.98
HEMP7AT	91.68	268.67	357.59	20.41
HEMP5HT	94.20	311.01	358.84	15.73
HEMP7HT	96.72	301.81	356.75	17.67

Table 6 DTG peaks of the fiber samples

	HEMP0	HEMP5AT	HEMP5HT	HEMP7AT	HEMP7HT
T_{max} (°C)	354.65	357.59	359.68	358.42	358.84

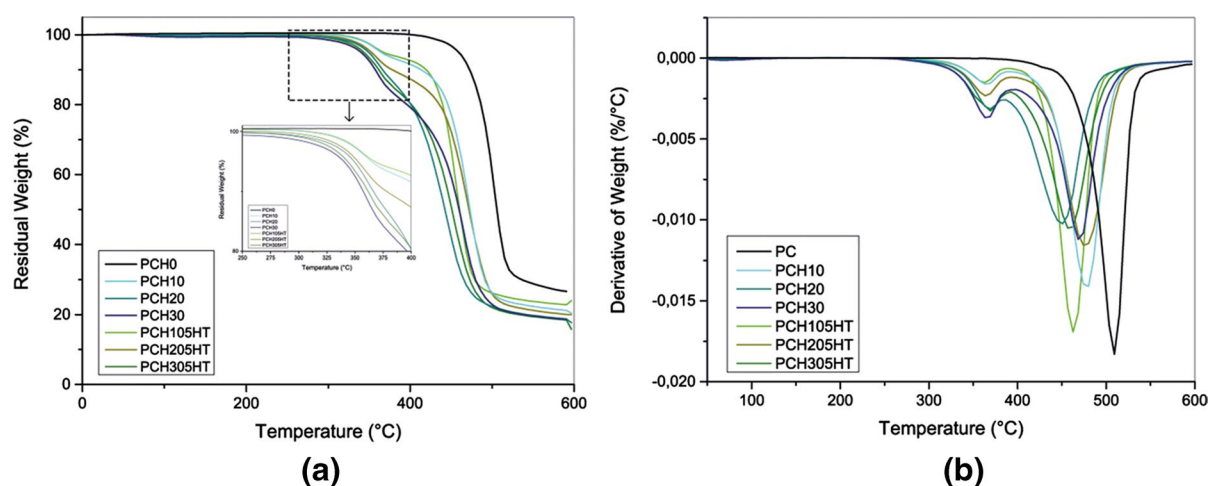


Fig. 7 TGA (a) and DTG (b) thermograms of the composites

Table 7 Heat-induced mass loss because of the TGA analysis of composite samples

Sample	5% Weight Loss (°C)	10% Weight Loss (°C)	50% Weight Loss (°C)	600 °C Residue (%)
PC	465.37	478.37	511.51	26.52
PCH10	370.58	419.12	478.64	21.13
PCH20	355.07	371.43	448.18	18.72
PCH30	345.84	363.04	465.37	18.53
PCH105HT	373.10	425.53	466.21	22.73
PCH205HT	373.10	384.43	477.53	19.98
PCH305HT	349.20	367.65	456.56	18.40

According to Oza et al. (2014), the DTG curves of PLA/Hemp composites show higher temperature values when reinforced with NaOH-treated fibers than when reinforced with untreated fibers (Oza et al. 2014). This increase was also observed in the PCH105HT, PCH205HT, and PCH305HT samples (see Table 7.). Lu and Oza (2013) reported that the TGA analysis of HDPE/ alkali hemp composites treated with NaOH showed that alkaline-treated fibers lost weight at higher temperatures than untreated fibers (Lu and Oza 2013). Similar results were obtained in the TGA analysis of alkali treated PCH105HT, PCH205HT, and PCH305HT samples. In the study by Lu and Oza (2013), TGA analysis of PLA/ alkali hemp composites treated with NaOH showed that alkali-treated fibers lost weight at higher temperatures than untreated fibers, and the weight loss due to temperature increased as the fiber ratio increased (Lu and Oza 2013). Similar results were obtained in the TGA analysis of alkali-treated PCH105HT, PCH205HT, and PCH305HT samples. Faulstich de Paiv and Frollini (2006) found that the TGA analysis of PC/ alkali sisal fiber composites showed that alkali-treated fibers lost weight at higher temperatures than untreated fibers (Faulstich de Paiv and Frollini 2006). Similar results were obtained in the TGA analysis of alkaline-treated PCH105HT, PCH205HT, and PCH305HT samples. Threepopnatkul et al. (2009), the TGA analysis of PC/PALF (pineapple leaf fiber) fiber composites alkaline treated with NaOH showed that the thermal strength decreases as the fiber ratio increases. Composites with all fiber ratios have lower thermal strength than pure PC composites. In addition, while only one degradation stage was observed for pure PC, the number of stages increased to three for fiber-added composites (Threepopnatkul et al. 2009). These results were also found in the TGA analysis

of the PCH105HT, PCH205HT, and PCH305HT samples.

When the thermal stability of the composites reinforced with hemp fiber and, natural fiber used to reinforce PC in the literature are examined, alkali-treated fiber included samples have better thermal strength than untreated samples. When we look at the TGA analysis performed within the scope of this study, this situation is valid for all alkali-treated samples at 5% and 10% weight loss, and the opposite situation is observed in alkali-treated composites, except for the PCH305HT sample at 50% weight loss temperature. Looking at the DTG peaks, the first degradation peak shows that the alkalis degrade at a lower temperature. In contrast, the second peak shows that only the PCH205HT sample degrades at a higher temperature. To explain this, SEM images will be analyzed to determine whether the alkali-treated samples blend better with pure PC.

DSC analysis

The DSC results for the composites incorporating alkali-treated and untreated fibers are outlined in Table 8. Examination of the T_g values derived from the DSC analysis revealed a general reduction in T_g values by adding fiber to the PC matrix. As the fiber ratio increases, the T_g value tends to decrease, indicating a plasticizing effect on the samples. Notably, composite samples reinforced with alkali-treated fibers exhibit higher T_g values than those reinforced with untreated fibers. This alignment with the laboratory production phase observations suggests a substantial reduction in the T_g value of composites reinforced with untreated fibers. The heightened plasticization is corroborated by the composite material's enhanced flow from the extruder device as a more fluid liquid and its ability

Table 8 DSC results of the composite samples

Sample	T_g (°C)	
	1st Stage	2nd Stage
PC	150.13	148.44
PCH10	138.18	146.74
PCH20	146.97	145.37
PCH30	146.03	143.98
PCH105HT	150.11	148.99
PCH205HT	149.72	146.74
PCH305HT	144.12	146.45

to be processed at lower temperatures using the 3D printer device. Reviewing the relevant literature, it was seen that changes in T_g values are intricately linked to the yield rate of alkaline treatment, a correlation consistent with the findings of this study.

According to Islam et al. (2010), as a result of DSC analysis applied to PLA/Hemp composites treated with NaOH, it was found that the addition of treated fiber decreased the T_g value compared with that of pure PLA composite. The T_g value of processed fiber is 61.20 °C, while pure PLA is 62.20 °C (Islam et al. 2010). The fiber ratio determined within the scope of their study is 30%, which is similar to that of the alkali-treated PCH305HT sample. According to Xiao et al. (2019), as a result of DSC analysis applied to PLA/Hemp composites using EGMA as a compatibilizer, the addition of fiber decreased the T_g value compared to pure PLA composite (Xiao et al. 2019). This result is similar to that of the untreated PCH10, PCH20, and PCH30 specimens. In the study conducted by Karslı and Aytac (2014), when the DSC analysis of PLA/PC/Flax composites treated with NaOH was examined, it was observed that the alkaline treated fibers increased the T_g value of the untreated composite. Although the T_g value decreased as the fiber ratio increased in the study, the T_g value for each fiber ratio was higher than those for PLA/PC and untreated PLA/PC/linen composites (Karslı and Aytac 2014). The fiber ratios used in the study were 2%, 5%, and 10%, and this result is similar to that of the PCH105HT sample containing only 10% fiber. Faulstich de Paiv and Frollini (2006) found that the DSC analysis of PC/Sisal fiber composites treated with NaOH showed that the alkali-treated

fibers peaked at higher temperatures than the untreated fibers. In addition, although only an exothermic peak was observed in untreated fiber composites, both exothermic and endothermic peaks were observed in treated composites (Faulstich de Paiv and Frollini 2006). This result is similar to the fact that PCH105HT, PCH205HT, and PCH305HT specimens reinforced with alkali-treated hemp fibers have higher T_g values than untreated specimens.

Mechanical characteristics

Tensile tests were applied to at least three samples by forming PC composite filaments reinforced with alkali-treated and untreated hemp fibers using a 3D printer. The tensile test results of the PC composite reinforced with hemp fiber at different fiber ratios are shown in Fig. 8. According to the tensile test results, that the tensile strength of the composites decreases as the fiber ratio increases. In general, composites reinforced with alkali-treated fibers have higher tensile strength values than untreated ones. No significant decrease in the maximum tensile strength was observed when comparing the PCH105HT specimen with the pure PC specimen (see Table 9.). As a result of adding 10% hemp fiber, the tensile strength of pure PC decreased by less than 2%. This result coincides with the tensile value results obtained in the literature within the scope of the study on PLA/Hemp composites printed with a 3D printer. According to the tensile value results, although pure PLA had a higher value, there was no significant decrease with adding hemp fiber (Guessasma et al. 2019).

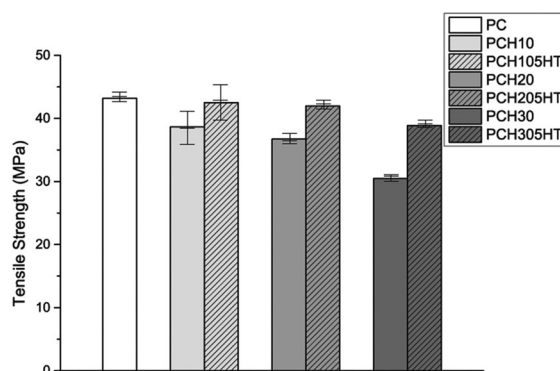
**Fig. 8** Tensile strength of the composites

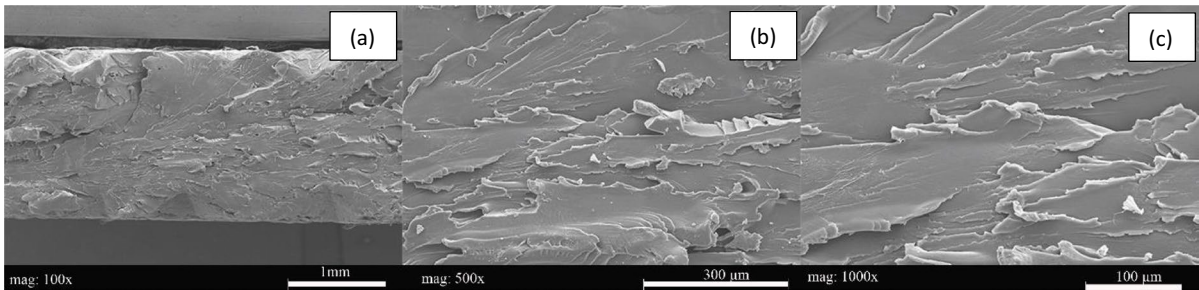
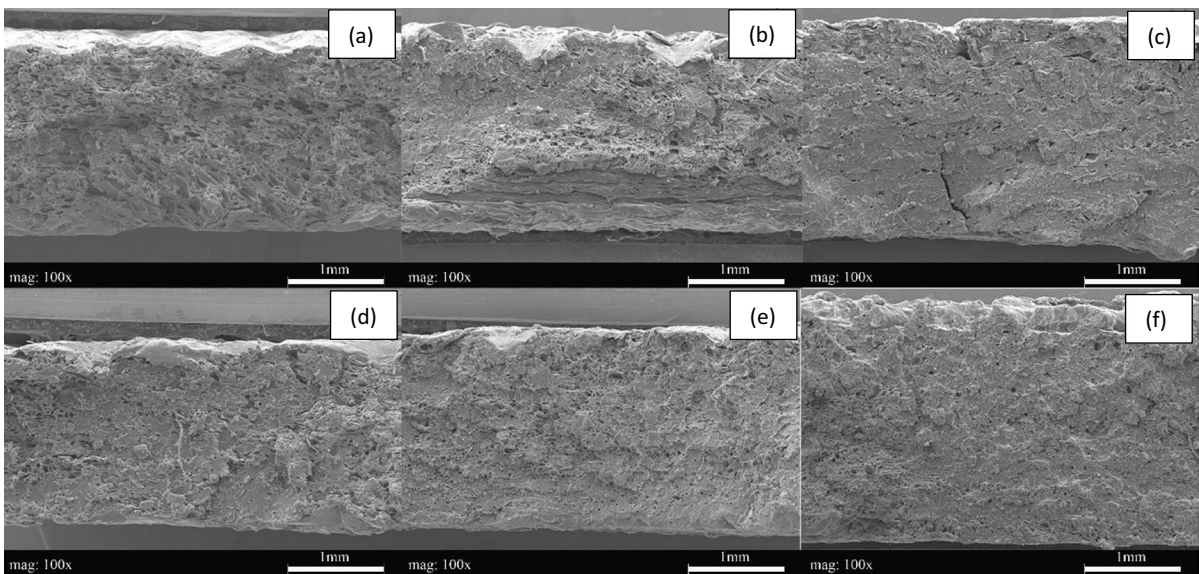
Table 9 Tensile strength of the composites

Sample	Tensile Strength (MPa)	Standard Deviation
PC	43.19	0.98
PCH10	38.66	3.67
PCH20	36.74	0.93
PCH30	30.46	0.74
PCH105HT	42.52	3.11
PCH205HT	41.98	0.60
PCH305HT	38.85	0.49

SEM analysis

SEM images taken from the fractured surfaces of the tensile test applied to pure PC formed by the FDM technique are shown in Fig. 9. When looking at pure PC, a porous structure appears (see Fig. 9 (a)). According to the information obtained from the SEM results of the composite produced with PC in the literature, the FDM technique can be associated with the presence of pores (Zhou et al. 2020).

SEM images taken from the fractured surfaces of the tensile test applied to alkali-treated and untreated hemp fiber-reinforced PC composites formed by the FDM technique are shown in Figs. 10, 11, and 12. In the untreated specimens, because of the weak

**Fig. 9** SEM images of pure PC. (a) 100x; (b) 500x, and (c) 1000x**Fig. 10** 100×SEM images of (a) PCH10, (b) PCH20, (c) PCH30, (d) PCH105HT, (e) PCH205HT, and (f) PCH305HT

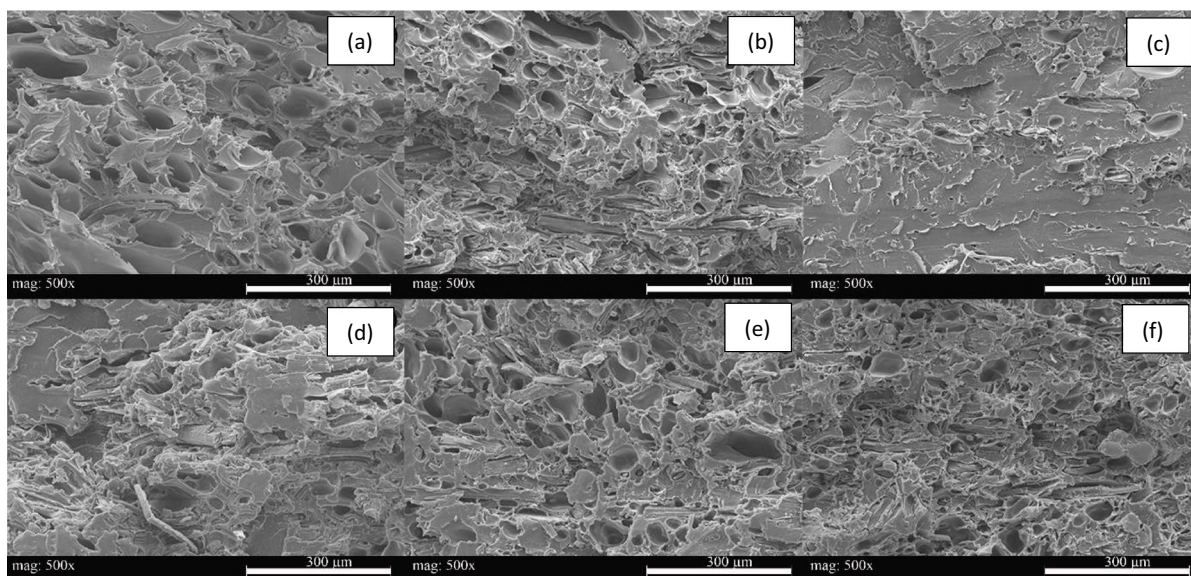


Fig. 11 500×SEM images of (a) PCH10, (b) PCH20, (c) PCH30, (d) PCH105HT, (e) PCH205HT, and (f) PCH305HT

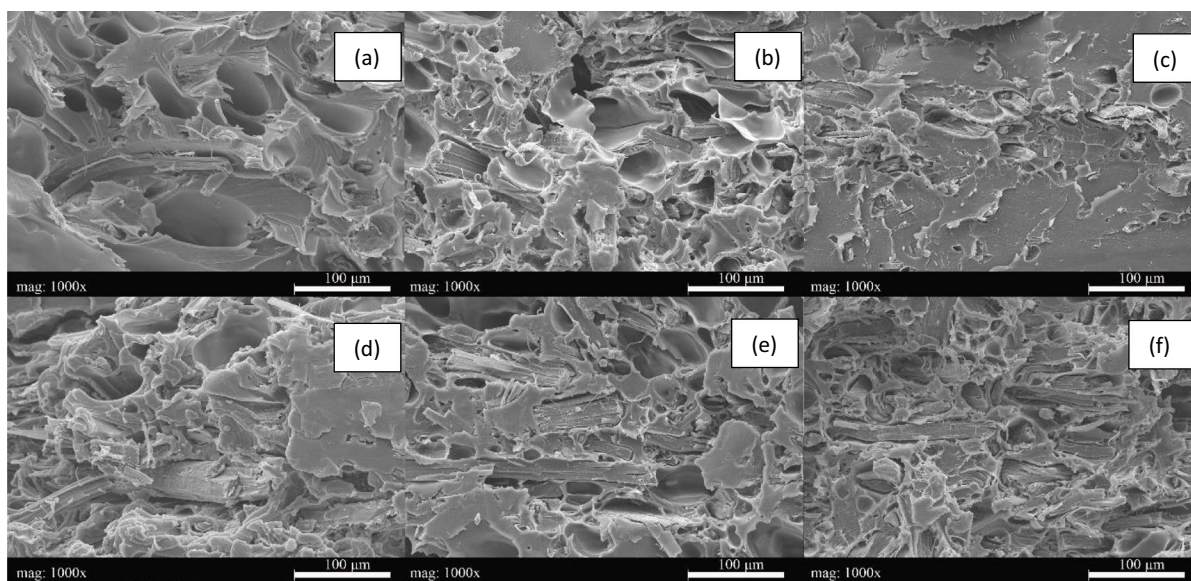


Fig. 12 1000×SEM images of (a) PCH10, (b) PCH20, (c) PCH30, (d) PCH105HT, (e) PCH205HT, and (f) PCH305HT

fiber-matrix interface bonding, a brittle fracture occurred in the composite, and there was a noticeable gap between the fiber and the matrix (see Fig. 10 (a), (b), and (c)). When looking at the PCH10 sample without alkali treatment, substances coated on the fiber surface can be observed. These substances may include pectin, lignin, and other impurities

(Sangappa Rao et al. 2014). Degradation occurs on the fiber surface, and the fibers start to come out of the matrix due to the weak fiber-matrix interface bond (see Fig. 11 (a), (b), (c)). Untreated hemp fibers begin to emerge from the matrix because of a weak interface bond. This is similar to studies in the literature (Bhoopathi and Ramesh 2020). As can be seen

from the SEM analysis, better fiber-matrix interface bonding was realized in the alkali-treated fibers. This is due to removing pectin, lignin, wax, and oils, as supported by the FTIR results. At the same time, the alkali-treated fibers have a fibrillated, rougher surface (see Fig. 12 (d), (e), and (f)). These results are similar to the SEM results obtained from the alkaline treatment of hemp fibers in the literature (Aruan Efendy and Pickering 2014; Kabir et al. 2013; Suardana et al. 2011). At the same time, the alkaline treatment of plant-based natural fibers resulted in a rougher surface, which is similar to the findings of previous studies (Karsli and Aytac 2014; Yan et al. 2012). The pores in the specimen are less than those in the composite specimens reinforced with untreated fiber. This reduction is due to wrapping the fibers with the matrix material, which results in a better fiber-matrix interface bond. The composites reinforced with NaOH alkali-treated hemp fibers have a less porous structure and better fiber-matrix interface bonding than the untreated ones. These results are similar to those reported in the literature (Bhoopathi and Ramesh 2020; Oliveira et al. 2021).

As supported by studies in the literature,

- Composites reinforced with alkali-treated fibers are more homogeneous and less porous than those reinforced with untreated fibers.
- As the porous structure decreases, the composites become stronger.
- These results are similar to the tensile test results.
- Alkali treatment provided fullness at the endpoint of the fibers. This fullness increases the stiffness and coincides with the tensile test results.
- Alkali treatment made the fiber surface smoother. This provides a better interface bond with the matrix material.
- In composites reinforced with alkali-treated fibers, fiber distribution is more homogeneous, and fiber surface breaks and distortions are less common than in untreated composite samples.

Conclusion

This article highlights the thermal, chemical, mechanical, and morphological properties of an alkali-treated hemp fiber-reinforced PC composite that can be formed with a 3D printer for architectural

applications. FTIR and TGA analyses were performed to determine the optimum alkali treatment for the fibers. The FTIR spectrum results showed that lignin was completely removed by applying 5% and 7% NaOH/pure water solutions under AT and HT conditions. Methylene groups, pectin, methyl ester, and waxy structures were removed under 5HT and 7AT conditions. The highest increase in cellulose was determined to be 5HT. Alkali treatment removed excess wax and waxy substances from the surface and increased the surface roughness. In addition, alkaline treatment increased the -OH density peak and provided better interface bonding of the fibers with the matrix material. When the TGA analysis was studied, it was found that the samples processed at 5HT conditions started to experience mass loss at higher temperatures compared with the other samples. These results determined that the most optimum alkali treatment that can be applied to hemp fibers is at the 5HT condition.

Tensile tests, FTIR, TGA, DSC, and SEM analyses were performed to characterize the composites. The highest tensile strength was observed for alkali-treated 10% hemp fiber-reinforced PC composites (PCH105HT). Regarding the tensile strength value, the PCH105HT sample lost less than 2% compared with the pure PC sample, which is not a significant decrease (PC: 43.19 MPa, PCH105HT: 42.52 MPa). PC is a synthetic material that is not biodegradable. As a result, a more environmentally friendly material was obtained by adding hemp fiber to PC. Because there is no significant decrease in mechanical values, it is predicted to be a natural alternative to architectural applications where a PC is used. For example, it can be used in semi-structural structures such as furniture parts or various interior design applications. The FTIR spectrum results show that composites reinforced with alkali-treated hemp fiber bond better with PC than untreated ones. The TGA analysis shows that the 10% mass loss of the pure PC sample occurs at 478.38 °C, whereas the closest value is the PCH105HT sample at 425.53 °C. When the char residue at 600 °C is analyzed, it is seen that PC gives the highest value with 26.52% and PCH105HT sample with 22.73% compared to the others. The T_g values obtained from the DSC analysis determined that the pure PC sample could be processed at 148.44 °C and the PCH105HT sample at 148.99 °C. No significant increase was observed in the PCH105HT sample. A

significant decrease was observed in all samples reinforced with untreated fibers and in the alkali-treated samples containing 20% and 30% fibers. It was determined that the material was plasticized. These data coincide with the observation of ease of printing with the FDM method in the laboratory process. Looking at the SEM images, it was found that the fiber and matrix formed a better interfacial bond because of the alkaline treatment. Thus, the gaps between the fiber and the matrix were minimized, and the material was strengthened by providing better mechanical PC and hemp fiber locking. As a result, it was determined that the PC composite reinforced with a 10% weight ratio of hemp fibers processed under 5HT conditions (PCH105HT) did not significantly decrease mechanical and thermal properties compared with pure PC. For this reason, it is expected that it is a more natural, sustainable, and green alternative to architectural applications where a PC is used and that complex forms can be created thanks to its suitability for use in 3D printers.

Acknowledgments We thank the Kocaeli University BAP Coordination Unit for funding project FDK-2022-2923 within the scope of funding doctoral thesis projects.

Author contributions All authors wrote the main manuscript text and reviewed the manuscript.

Funding Open access funding provided by the Scientific and Technological Research Council of Türkiye (TÜBİTAK). The Kocaeli University BAP Coordination Unit funded this study within the scope of 'funding doctoral thesis projects.' Project no: FDK-2022–2923.

Data availability This declaration is not applicable.

Declarations

The authors are conducting a doctoral thesis within the scope of this study.

Ethical approval Ethical approvals are not applicable.

Competing interest The authors declare that they have no known competing financial interests or personal relationships that could have influenced the work reported in this paper.

Open Access This article is licensed under a Creative Commons Attribution 4.0 International License, which permits use, sharing, adaptation, distribution and reproduction in any medium or format, as long as you give appropriate credit to the original author(s) and the source, provide a link to the Creative Commons licence, and indicate if changes were made. The

images or other third party material in this article are included in the article's Creative Commons licence, unless indicated otherwise in a credit line to the material. If material is not included in the article's Creative Commons licence and your intended use is not permitted by statutory regulation or exceeds the permitted use, you will need to obtain permission directly from the copyright holder. To view a copy of this licence, visit <http://creativecommons.org/licenses/by/4.0/>.

References

- Alves C, Ferrão PMC, Silva AJ, Reis LG, Freitas M, Rodrigues LB, Alves DE (2010) Ecodesign of automotive components making use of natural jute fiber composites. *J Clean Prod* 18(4):313–327. <https://doi.org/10.1016/J.JCLEPRO.2009.10.022>
- Amaducci S, Scordia D, Liu FH, Zhang Q, Guo H, Testa G, Cosentino SL (2015) Key cultivation techniques for hemp in Europe and China. *Ind Crops Prod* 68:2–16. <https://doi.org/10.1016/j.indcrop.2014.06.041>
- Apaydin-Varol E, Polat S, Putun AE (2014) Pyrolysis kinetics and thermal decomposition behavior of polycarbonate-a TGA-FTIR study. *Therm Sci* 18(3):833–842. <https://doi.org/10.2298/TSCI1403833A>
- Aruan Efendy MG, Pickering KL (2014) Comparison of harakeke with hemp fibre as a potential reinforcement in composites. *Compos Part A Appl Sci* 67:259–267. <https://doi.org/10.1016/j.compositesa.2014.08.023>
- Ayrlimis N, Jarusombuti S, Fueangvivat V, Bauchongkol P, White RH (2011) Coir fiber reinforced polypropylene composite panel for automotive interior applications. *Fibers Polym* 12(7):919–926. <https://doi.org/10.1007/s12221-011-0919-1>
- Azwa ZN, Yousif BF (2013) Characteristics of kenaf fibre/epoxy composites subjected to thermal degradation. *Polym Degrad Stab* 98(12):2752–2759. <https://doi.org/10.1016/J.POLYMDEGRADSTAB.2013.10.008>
- Bhoopathi R, Ramesh M (2020) Influence of Eggshell Nanoparticles and Effect of Alkalization on Characterization of Industrial Hemp Fibre Reinforced Epoxy Composites. *J Polym Environ* 28(8):2178–2190. <https://doi.org/10.1007/s10924-020-01756-1>
- Bourmaud A, Baley C (2007) Investigations on the recycling of hemp and sisal fibre reinforced polypropylene composites. *Polym Degrad Stab* 92(6):1034–1045. <https://doi.org/10.1016/j.polymdegradstab.2007.02.018>
- Chua CK, Leong KF, Lim CS (2003) Rapid Prototyping. *World Sci*. <https://doi.org/10.1142/5064>
- Domingo Espin M, Puigoriol Forcada JM, Garcia Granada AA, Llumà J, Borros S, Reyes G (2015) Mechanical property characterization and simulation of fused deposition modeling Polycarbonate parts. *Mater Des* 83:670–677. <https://doi.org/10.1016/j.matdes.2015.06.074>
- Faruk O, Bledzki AK, Fink HP, Sain M (2012) Biocomposites reinforced with natural fibers: 2000–2010. *Prog Polym Sci* 37(11):1552–1596. <https://doi.org/10.1016/j.propolymsci.2012.04.003>

- Faulstich de Paiv JM, Frollini E (2006) Unmodified and Modified Surface Sisal Fibers as Reinforcement of Phenolic and Lignophenolic Matrices Composites. *Macromol Mater Eng* 291(4):405–417. <https://doi.org/10.1002/mame.200500334>
- Guessasma S, Belhabib S, Nouri H (2019) Understanding the microstructural role of bio-sourced 3D printed structures on the tensile performance. *Polym Test*. <https://doi.org/10.1016/j.polymertesting.2019.105924>
- Haghighi Yazdi M, Lee Sullivan P (2015) FTIR analysis of a polycarbonate blend after hygrothermal aging. *J Appl Polym Sci* 132(3). <https://doi.org/10.1002/app.41316>
- Hapuarachchi TD, Peijs T (2010) Multiwalled carbon nanotubes and sepiolite nanoclays as flame retardants for polylactide and its natural fibre reinforced composites. *Compos Part A Appl Sci* 41(8):954–963. <https://doi.org/10.1016/j.compositesa.2010.03.004>
- Hashemi Sanatgar R, Campagne C, Nierstrasz V (2017) Investigation of the adhesion properties of direct 3D printing of polymers and nanocomposites on textiles: Effect of FDM printing process parameters. *Appl Surf Sci* 403:551–563. <https://doi.org/10.1016/j.apsusc.2017.01.112>
- Hu R, Lim JK (2007) Fabrication and mechanical properties of completely biodegradable hemp fiber reinforced polylactic acid composites. *J Compos Mater* 41(13):1655–1669. <https://doi.org/10.1177/0021998306069878>
- Islam MS, Pickering KL, Foreman NJ (2010) Influence of alkali treatment on the interfacial and physico-mechanical properties of industrial hemp fibre reinforced polylactic acid composites. *Compos Part A Appl Sci* 41(5):596–603. <https://doi.org/10.1016/j.compositesa.2010.01.006>
- Jayaramudu J, Reddy GSM, Varaprasad K, Sadiku ER, Ray SS, Rajulu AV (2013) Effect of Alkali Treatment on the Morphology and Tensile Properties of Cordia Dichotoma Fabric/Polycarbonate Composites. *Adv Polym Technol*. <https://doi.org/10.1002/adv.21349>
- JhanjiDhir Y (2022) Natural Fibers: The Sustainable Alternatives for Textile and Non-Textile Applications. *IntechOpen, Natural Fiber*. <https://doi.org/10.5772/intechopen.106393>
- Juárez C, Guevara B, Valdez P, Durán Herrera A (2010) Mechanical properties of natural fibers reinforced sustainable masonry. *Constr Build Mater* 24(8):1536–1541. <https://doi.org/10.1016/J.CONBUILDMAT.2010.02.007>
- Kabir MM, Wang H, Lau KT, Cardona F, Aravinthan T (2012) Mechanical properties of chemically-treated hemp fibre reinforced sandwich composites. *Compos B Eng* 43(2):159–169. <https://doi.org/10.1016/j.compositesb.2011.06.003>
- Kabir MM, Wang H, Lau KT, Cardona F (2013) Effects of chemical treatments on hemp fibre structure. *Appl Surf Sci* 276:13–23. <https://doi.org/10.1016/j.apsusc.2013.02.086>
- Kandola BK, Mistik SI, Pornwannachai W, Horrocks AR (2021) Effects of water and chemical solutions ageing on the physical, mechanical, thermal and flammability properties of natural fibre-reinforced thermoplastic composites. *Molecules* 26(15):4581. <https://doi.org/10.3390/molecules26154581>
- Karsli NG, Aytac A (2014) Properties of alkali treated short flax fiber reinforced poly(lactic acid)/polycarbonate composites. *Fibers Polym* 15(12):2607–2612. <https://doi.org/10.1007/s12221-014-2607-4>
- Kozłowski R, Władysław Przybylak M (2006) Composites reinforced with lignocellulosic fibres. In *Advances and Challenges in Biocomposites: Proceedings of the 8th Pacific Rim Bio-Based Composites Symposium*, Kuala Lumpur
- Kozłowski R, Władysław Przybylak M (2008) Flammability and fire resistance of composites reinforced by natural fibers. *Polym Adv Technol* 19(6):446–453. <https://doi.org/10.1002/pat.1135>
- Kreiger M, Pearce JM (2013) Environmental Life Cycle Analysis of Distributed Three-Dimensional Printing and Conventional Manufacturing of Polymer Products. *ACS Sustain Chem Eng* 1(12):1511–1519. <https://doi.org/10.1021/sc400093k>
- Ku H, Wang H, Pattarachaiyakoop N, Trada M (2011) A review on the tensile properties of natural fiber reinforced polymer composites. *Compos B Eng* 42(4):856–873. <https://doi.org/10.1016/J.COMPOSITESB.2011.01.010>
- Li X, Panigrahi S, Tabil LG (2009) A study on flax fiber-reinforced polyethylene biocomposites. *Appl Eng Agric* 25(4):525–531. <https://doi.org/10.13031/2013.27454>
- Liu M, Thygesen A, Summerscales J, Meyer AS (2017) Targeted pre-treatment of hemp bast fibres for optimal performance in biocomposite materials: A review. *Ind Crops Prod* 108:660–683. <https://doi.org/10.1016/j.indcrop.2017.07.027>
- Lu N, Oza S (2013) Thermal stability and thermo-mechanical properties of hemp-high density polyethylene composites: Effect of two different chemical modifications. *Compos B Eng* 44(1):484–490. <https://doi.org/10.1016/j.compositesb.2012.03.024>
- Maheswari CU, Reddy KO, Muzenda E, Rajulu AV (2012) Tensile and Thermal Properties of Polycarbonate-Coated Tamarind Fruit Fibers. *Int J Polym Anal* 17(8):578–589. <https://doi.org/10.1080/1023666X.2012.718527>
- Mohammed MI, Mohan M, Das A, Johnson M, Singh Badwal P, McLean D, Gibson I (2017) A low carbon footprint approach to the reconstitution of plastics into 3D-printer filament for enhanced waste reduction. *KnE Eng* 2(2):234. <https://doi.org/10.18502/keg.v2i2.621>
- Mohanty AK, Misra M, Drzal LT (2001) Surface modifications of natural fibers and performance of the resulting biocomposites: An overview. *Compos Interfaces* 8(5):313–343. <https://doi.org/10.1163/156855401753255422>
- Nishino T, Hirao K, Kotera M, Nakamae K, Inagaki H (2003) Kenaf reinforced biodegradable composite. *Compos Sci Technol* 63(9):1281–1286. [https://doi.org/10.1016/S0266-3538\(03\)00099-X](https://doi.org/10.1016/S0266-3538(03)00099-X)
- Oliveira MAS, Pickering KL, Sunny T, Lin RJT (2021) Treatment of hemp fibres for use in rotational moulding. *J Polym Res* 28(2):53. <https://doi.org/10.1007/s10965-021-02414-3>
- Oujai S, Shanks RA (2005) Composition, structure and thermal degradation of hemp cellulose after chemical treatments. *Polym Degrad Stab* 89(2):327–335. <https://doi.org/10.1016/j.polymdegradstab.2005.01.016>
- Oza S, Ning H, Ferguson I, Lu N (2014) Effect of surface treatment on thermal stability of the hemp-PLA composites:

- Correlation of activation energy with thermal degradation. *Compos B Eng* 67:227–232. <https://doi.org/10.1016/j.compositesb.2014.06.033>
- Panthapulakkal S, Sain M (2013) Isolation of Nano Fibres from Hemp and Flax and Their Thermoplastic Composites. *Polym Plast Technol Eng* 2:1
- Pickering KL, Sawpan MA, Jayaraman J, Fernyhough A (2011) Influence of loading rate, alkali fibre treatment and crystallinity on fracture toughness of random short hemp fibre reinforced polylactide bio-composites. *Compos Part A Appl Sci* 42(9):1148–1156. <https://doi.org/10.1016/j.compositesa.2011.04.020>
- Pracella M, Haque MU, Alvarez V (2010) Functionalization, Compatibilization and Properties of Polyolefin Composites with Natural Fibers. *Polym J* 2(4):554–574. <https://doi.org/10.3390/polym2040554>
- Rachini A, Le Troedec M, Peyratout C, Smith A (2009) Comparison of the thermal degradation of natural, alkali-treated and silane-treated hemp fibers under air and an inert atmosphere. *J Appl Polym Sci* 112(1):226–234. <https://doi.org/10.1002/app.29412>
- Reddy BM, Mohana Reddy YV, Mohan Reddy BC, Reddy RM (2020) Mechanical, morphological, and thermogravimetric analysis of alkali-treated *Cordia-Dichotoma* natural fiber composites. *J Nat Fibers* 17(5):759–768. <https://doi.org/10.1080/15440478.2018.1534183>
- Saba N, Paridah MT, Jawaid M (2015) Mechanical properties of kenaf fibre reinforced polymer composite: A review. *Constr Build Mater* 76:87–96. <https://doi.org/10.1016/j.conbuildmat.2014.11.043>
- Saba N, Jawaid M, Alothman OY, Paridah MT (2016) A review on dynamic mechanical properties of natural fibre reinforced polymer composites. *Constr Build Mater* 106:149–159. <https://doi.org/10.1016/j.conbuildmat.2015.12.075>
- Sangappa Rao BL, Asha S, Kumar RM, Somashekar R (2014) Physical, chemical, and surface properties of alkali-treated Indian hemp fibers. *Compos Interfaces* 21(2):153–159. <https://doi.org/10.1080/15685543.2013.855485>
- Sanjay MR, Madhu P, Jawaid M, Senthamaraiannan P, Senthil S, Pradeep S (2018) Characterization and properties of natural fiber polymer composites: A comprehensive review. *J Clean Prod* 172:566–581. <https://doi.org/10.1016/j.jclepro.2017.10.101>
- Sawpan MA, Pickering KL, Fernyhough A (2011) Improvement of mechanical performance of industrial hemp fibre reinforced polylactide biocomposites. *Compos Part A Appl Sci* 42(3):310–319. <https://doi.org/10.1016/j.compositesa.2010.12.004>
- Suardana NPG, Piao Y, Lim JK (2011) Mechanical properties of hemp fibers and hemp/PP composites: effects of the chemical surface treatment. *Mater Phys Mech* 11:1–8
- Sunny T, Pickering KL, Lim SH (2020) Alkali treatment of hemp fibres for the production of aligned hemp fibre mats for composite reinforcement. *Cellulose* 27(5):2569–2582. <https://doi.org/10.1007/s10570-019-02939-3>
- Szostak M, Tomaszewska N, Kozłowski R (2019) Mechanical and Thermal Properties of Rotational Molded PE/Flax and PE/Hemp Composites. In: *Energy Transfer and Dissipation in Plasma Turbulence*, 1st edn, Springer, 495–506. https://doi.org/10.1007/978-3-030-16943-5_42
- Taşdemir M, Koçak D, Usta İ, Akalin M, Merdan N (2008) Properties of Recycled Polycarbonate/Waste Silk and Cotton Fiber Polymer Composites. *Int J Polym Mater* 57(8):797–805. <https://doi.org/10.1080/00914030802089138>
- Thakur VK, Thakur MK, Pappu A (2017) Hybrid polymer composite materials: Applications. *Hybrid Polymer Composite Materials*, 1st edn. Elsevier, Amsterdam, pp 19–28
- Threepopnatkul P, Kaerkitcha N, Athipongarporn N (2009) Effect of surface treatment on performance of pineapple leaf fiber–polycarbonate composites. *Compos B Eng* 40(7):628–632. <https://doi.org/10.1016/j.compositesb.2009.04.008>
- Victoria Santos N, Cardoso D, Santos N, Cardoso D (2022) 3D Printing polymer composites reinforced with continuous vegetable fibers. In: *6 th Brazilian Conference on Composite Materials*. Tiradantes, 1–6.
- Vinyas M, Athul SJ, Harursampath D, Nguyen Thoi T (2019) Experimental evaluation of the mechanical and thermal properties of 3D printed PLA and its composites. *Mater Res Express* 6(11):115301. <https://doi.org/10.1088/2053-1591/ab43ab>
- Wang B, Panigrahi S, Tabil L, Crerar WJ, Powell T, Kolybaba M, Sokhansanj S (2003) Flax fiber-reinforced thermoplastic composites. *Journal The Society for Eng. in Agricultural, Food, and Biological Systems*, Dep. of Agricultural and Bioresource Eng Univ of Saskatchewan 57
- Williams CB, Ivanova O (2011) Could 3D Printing Change the World? Technologies, Potential, and Implications of Additive Manufacturing. *Jstor*. <https://www.jstor.org/stable/pdf/resrep03564.pdf?refreqid=excelsior%3Ae8c09a61e0e656681bbbf51314277897&seq=1>. Accessed 23 August 2023
- Wimonsong W, Threepopnatkul P, Kulsethanchalee C (2012) Thermal conductivity and mechanical properties of wood sawdust/ polycarbonate composites. *Mater Sci Forum* 714:139–146. <https://doi.org/10.4028/www.scientific.net/MSF.714.139>
- Wirawan R, Zainudin ES, Sapuan SM (2009) Mechanical properties of natural fibre reinforced PVC composites: A review. *Sains Malays* 38(4):531–535
- Xiao X, Chevali VS, Song P, He D, Wang H (2019) Polylactide/hemp hurd biocomposites as sustainable 3D printing feedstock. *Compos Sci Technol* 184:107887. <https://doi.org/10.1016/j.compscitech.2019.107887>
- Yan L, Chouh N, Yuan X (2012) Improving the mechanical properties of natural fibre fabric reinforced epoxy composites by alkali treatment. *J Reinf Plast Comp* 31(6):425–437. <https://doi.org/10.1177/0731684412439494>
- Yan L, Kasal B, Huang L (2016) A review of recent research on the use of cellulosic fibres, their fibre fabric

- reinforced cementitious, geo-polymer and polymer composites in civil engineering. *Compos B Eng* 92:94–132. <https://doi.org/10.1016/J.COMPOSITESB.2016.02.002>
- Zafar MF, Siddiqui MA (2020) Effect of filler loading and size on the mechanical and morphological behaviour of natural fibre-reinforced polystyrene composites. *Adv Mater Process Technol* 1–13. <https://doi.org/10.1080/2374068X.2020.1793261>.
- Zhang J, Koubaa A, Xing D, Liu W, Wang H, Wang XM, Wang Q (2020) High-performance lignocellulose/polycarbonate biocomposites fabricated by in situ reaction: Structure and properties. *Compos Part A Appl Sci* 138:106068. <https://doi.org/10.1016/J.COMPOSITESA.2020.106068>
- Zhang J, Koubaa A, Xing D, Godard F, Li P, Tao Y, Wang XM, Wang H (2021) Fire Retardancy, Water Absorption, and Viscoelasticity of Borated Wood—Polycarbonate Biocomposites. *Polym J* 13(14):2234. <https://doi.org/10.3390/polym13142234>
- Zhou Y, Zou J, Wu H, Xu B (2020) Balance between bonding and deposition during fused deposition modeling of polycarbonate and acrylonitrile-butadiene-styrene composites. *Polym Compos* 41(1):60–72. <https://doi.org/10.1002/pc.25345>

Publisher's Note Springer Nature remains neutral with regard to jurisdictional claims in published maps and institutional affiliations.